Reprinted from JOURNAL OF COMPUTATIONAL PHYSICS
All Rights Reserved by Academic Press, New York and London

Vol. 30, No. 2, February 1979
Printed in Belgium

Numerical Solution of a Nonlinear Hyperbolic Equation by the Random Choice Method

PAUL CONCUS AND WLODZIMIERZ PROSKUROWSKI

Lawrence Berkeley Laboratory, University of California, Berkeley, California 94720

Received August 11, 1977; revised March 9, 1978

The numerical solution of a nonlinear hyperbolic equation not fulfilling the strict nonlinearity condition is considered. A solution procedure is developed based on the random choice method, which permits the sharp tracking of discontinuities. As an illustration, an application to the two-phase flow of petroleum in underground reservoirs is presented.

1. INTRODUCTION

In recent papers Chorin [2, 3] has presented a random choice method (RCM) for obtaining the numerical solution of systems of nonlinear hyperbolic equations, in particular those arising in gasdynamics. It is well known that, in general, the solution of such equations develop discontinuities even for smooth initial data. Chorin's method, based on an existence proof due to Glimm [5], is designed particularly for the tracking of these discontinuities, a task that conventional numerical methods often perform poorly.

The purpose of our paper is to present a numerical method based on RCM for a nonlinear hyperbolic equation of special type, which arises in the study of two-phase immiscible flow and does not fulfill the strict nonlinearity condition [7]. A particular application to the flow of petroleum in underground reservoirs is considered, and numerical examples are given for the Buckley–Leverett equation.

2. DESCRIPTION OF THE RANDOM CHOICE METHOD

Consider a single nonlinear hyperbolic equation in one space dimension

$$\frac{\partial u}{\partial t} + \frac{\partial}{\partial x} f(u) = 0. \tag{1}$$

For the problems we shall study, $f(u)$ is twice continuously differentiable, although the RCM algorithm may be applied to cases for which $f(u)$ is not this smooth [2, 3]. The RCM algorithm obtains an approximation to the values of $u(x, t)$ at the spatial points $x_i = ih$, $i = 0, \pm 1, \ldots$ at times $t_j = jk$, $j = 0, 1, \ldots$ and at the points $x_{i+\frac{1}{2}} =$

0021-9991/79/020153-14$02.00/0

$(i + \frac{1}{2})h$ at times $t_{j+\frac{1}{2}} = (j + \frac{1}{2})k$, where h and k are the space and time increments, respectively. Denote the discrete approximation to $u(ih, jk)$ by u_i^j.

The RCM algorithm consists of a sequence of steps that advances the solution forward in time from given initial values u_i^0, $i = 0, \pm 1, \ldots$. Each time step from t_j to t_{j+1} consists of two half-steps, one from t_j to $t_{j+\frac{1}{2}}$ followed by one from $t_{j+\frac{1}{2}}$ to t_{j+1}. We consider the first half-step from t_j to $t_{j+\frac{1}{2}}$, the other one is analogous.

At time t_j, the RCM algorithm takes $u(x, t_j)$ to be approximated by the piecewise constant function equal to u_i^j in each interval $(i - \frac{1}{2})h < x \leqslant (i + \frac{1}{2})h$. Then, the exact (weak) solution of (1) with this function as initial data is constructed analytically for $t_j \leqslant t \leqslant t_{j+\frac{1}{2}}$, under the assumption that $t_{j+\frac{1}{2}} - t_j$ is not too large. This construction is carried out by solving, for each i, the Riemann initial value problem

$$\frac{\partial v}{\partial t} + \frac{\partial}{\partial x} f(v) = 0 \tag{2}$$

for $t > t_j$, with

$$v(x, t_j) = \begin{cases} u_i^j, & \text{for } x \leqslant (i + \frac{1}{2})h, \\ u_{i+1}^j, & \text{for } x > (i + \frac{1}{2})h. \end{cases} \tag{3}$$

In general $u_i^j \neq u_{i+1}^j$, so that there is a discontinuity in the initial data (3) at $x = (i + \frac{1}{2})h$, from which a wave propagates as t increases. Denote

$$a(u) = \frac{df(u)}{du},$$

so that (1) is equivalent to

$$\frac{\partial u}{\partial t} + a(u) \frac{\partial u}{\partial x} = 0.$$

Then if the Courant condition

$$\frac{k}{h} \max_u | a(u)| < 1 \tag{4}$$

is imposed, the waves propagated from the discontinuity of each Riemann problem do not intersect. Thus, if (4) is satisfied, the solutions of the Riemann problems (2, 3) can be joined together to form the solution to (1) at $t = t_{j+\frac{1}{2}}$ for the initial piecewise constant data at $t = t_j$.

By means of a random choice procedure, this solution is then sampled in an interval $[-\frac{1}{2}h, \frac{1}{2}h]$ about each point $(i + \frac{1}{2})h$ to obtain the values to be assigned to $u_{i+\frac{1}{2}}^{j+\frac{1}{2}}$, $i = 0, \pm 1, \ldots$. If $v(x, t)$ is the solution of (2, 3), then the value assigned to $u_{i+\frac{1}{2}}^{j+\frac{1}{2}}$ is

$$u_{i+\frac{1}{2}}^{j+\frac{1}{2}} = v([i + \tfrac{1}{2} + \tfrac{1}{2}\theta_{j+\frac{1}{2}}]h, [j + \tfrac{1}{2}]k),$$

where $\theta_{j+\frac{1}{2}}$ is sampled at random from a distribution on the interval $[-1, 1]$.

An analogous procedure is used to advance from time $t_{j+\frac{1}{2}}$ to time t_{j+1}, and the entire process is carried out repeatedly for increasing values of j.

Glimm [5] proved the convergence of this method on the interval $-\infty < x < \infty$ assuming strict nonlinearity of (1) (i.e., $d^2f/du^2 \neq 0$) and small oscillations of the initial data. Later, Kuznecov and Tupčiev [6] removed the restriction of strict nonlinearity. For our problem the assumption of small oscillations may not hold; however, computational evidence indicates that even for such problems, and other problems not satisfying the restrictions of the proofs, the RCM algorithm converges [2]. In [2, 3] Chorin develops the treatment of boundary conditions and the sampling procedures for θ that are crucial for the numerical success of the method. A proper sampling procedure ensures not only that the u_i^j are valid approximations to the solution values at large times, but at intermediate times as well.

The RCM algorithm is unconditionally stable, approaches being first order accurate, and propagates discontinuities (shocks) sharply without dissipation. A small amount of statistical uncertainty is introduced into the solution, but this uncertainty is generally entirely acceptable within the accuracy limits imposed by the discretization. The introduction of discontinuities by the method is not unnatural since, in general, the exact solution of (1) develops discontinuities in finite time even for smooth initial data.

3. Solution of a Riemann Problem

Success in applying the RCM algorithm depends upon the possibility of solving the required set of Riemann problems, and upon doing so efficiently. We indicate how this can be done for (2, 3) for the $f(u)$ under consideration.

For notational convenience we rephrase the Riemann problem (2, 3) as follows. Denote by u_L the initial value u_i^j to the left of $x = (i + \frac{1}{2})h$ and denote by u_R the initial value u_{i+1}^j to the right of $x = (i + \frac{1}{2})h$. Shift the origin to $([i + \frac{1}{2}]h, jk)$ to obtain a local system of coordinates. Then (3) becomes

$$v(x, 0) = \begin{cases} u_L, & x \leqslant 0, \\ u_R, & x > 0. \end{cases} \tag{5}$$

We consider in the following subsections the solution in the local coordinates of the Riemann problem (2, 5) for $t > 0$.

3.1. *Basic Results*

Our construction of the solution of the Riemann problem is based upon the following results, which can be found in [4, 7, 9], and elsewhere. If $u_L = u_R$, then the solution of (2, 5) is constant: $v(x, t) = u_L = u_R$. If $u_L \neq u_R$, then the initial discontinuity at $x = 0$, which separates the constant states u_L and u_R, will propagate as a centered expansion wave and/or a shock (which may be a contact discontinuity).

To obtain a unique weak solution of (2, 5), the following conditions must hold along any curve of discontinuity of $v(x, t)$. Let $v_- = \lim_{x \to x_-} v(x, t)$ and $v_+ = \lim_{x \to x_+} v(x, t)$ be the limiting values from the left and right, respectively, at the discontinuity. The following must hold (see, for example, [4]):

(i) (Rankine–Hugoniot jump condition) The curve of discontinuity is a straight line with slope

$$\frac{dx}{dt} = \frac{f(v_+) - f(v_-)}{v_+ - v_-};$$

and

(ii) (*E*-condition of Oleĭnik [9])

$$\frac{f(v_+) - f(v)}{v_+ - v} \leqslant \frac{f(v_+) - f(v_-)}{v_+ - v_-}$$

for any v between v_+ and v_-. Condition (ii) corresponds to the condition that the chord $l_{-,+}(v)$ joining $(v_-, f(v_-))$ and $(v_+, f(v_+))$,

$$l_{-,+}(v) = f(v_+) + \frac{f(v_+) - f(v_-)}{v_+ - v_-}(v - v_+),$$

satisfies

$$l_{-,+}(v) \geqslant f(v), \quad \text{if} \quad v_- > v_+,$$
$$l_{-,+}(v) \leqslant f(v), \quad \text{if} \quad v_+ > v_-,$$

for any v between v_- and v_+.

3.2. *Solution for a Particular* $f(u)$

In this paper our primary interest is in solving (1) for the particular functions $f(u)$ that arise in the study of two-phase immiscible flow in porous media, for example in the flow of petroleum in underground reservoirs. We assume, as usually holds for such cases, that $f(u)$ has exactly one inflection point u_I, that $a(u) = df(u)/du \geqslant 0$ in the domain of dependence, and that $a(u)$ has its maximum at $u = u_I$. The last two conditions are not essential; however, as they are the ones occurring in practice, we base our discussion below and Figs. 3–5 on them. The essential feature is the inflection in $f(u)$, which introduces a complexity not found in strictly nonlinear cases, for which d^2f/du^2 does not vanish.

Based on conditions (i) and (ii) of Section 3.1, we obtain the solution of the Riemann problem (2, 5) for the $f(u)$ under consideration as follows.

If $u_L \neq u_R$, let $S_{L,R}$ denote the slope of the chord $l_{L,R}(u)$ joining $(u_L, f(u_L))$ and $(u_R, f(u_R))$,

$$S_{L,R} = \frac{f(u_R) - f(u_L)}{u_R - u_L}.$$

We must distinguish between the following cases:

(I) The chord $l_{L,R}(u)$ does not cut the graph of $f(u)$ for any value of u between u_L and u_R. Then the value of $S_{L,R}$ lies between $a(u_L)$ and $a(u_R)$; and

(Ia) if $a(u_L) > a(u_R)$, the state $v = u_L$ is connected to the state $v = u_R$ by a shock propagating with speed $dx/dt = S_{L,R}$;

(Ib) if $a(u_L) < a(u_R)$, the state u_L is connected to u_R by an expansion wave.

(II) The chord $l_{L,R}(u)$ cuts the graph of $f(u)$ for some value of u between u_L and u_R. Then for our $f(u)$, $S_{L,R} > a(u_L)$ and $S_{L,R} > a(u_R)$. In accordance with (i) and (ii), two possibilities must be considered:

(IIa) If $u_L > u_R$, we construct the convex hull $H(u)$ to $f(u)$ in (u_R, u_L) (see Fig. 1).

(IIb) If $u_L < u_R$, we construct the concave hull $h(u)$ to $f(u)$ in (u_L, u_R) (see Fig. 2).

For either (IIa) or (IIb) let u_M be the point such that $S_{M,R} = a(u_M)$, where

$$S_{M,R} = \frac{f(u_R) - f(u_M)}{u_R - u_M}.$$

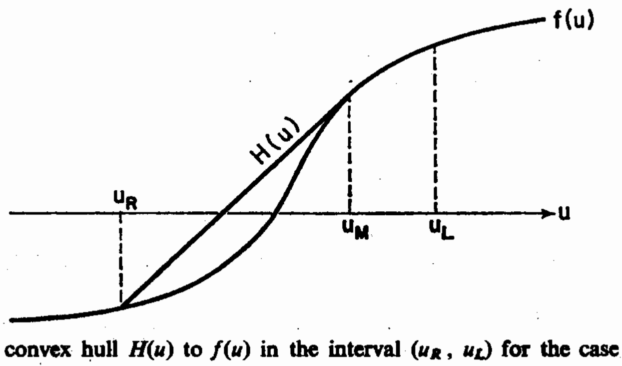

FIG. 1. The convex hull $H(u)$ to $f(u)$ in the interval (u_R, u_L) for the case $u_L > u_R$.

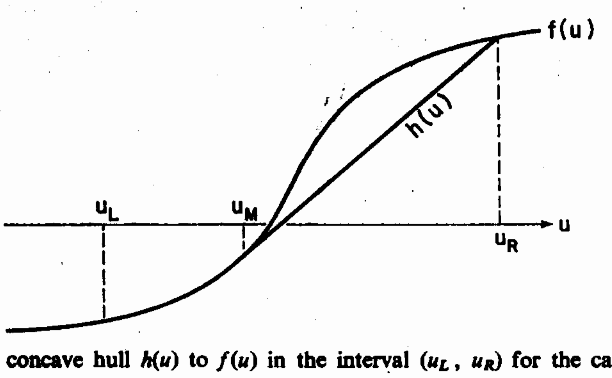

FIG. 2. The concave hull $h(u)$ to $f(u)$ in the interval (u_L, u_R) for the case $u_L < u_R$.

Then the state $v = u_L$ is connected to $v = u_M$ by an expansion wave, and $v = u_M$ is connected to $v = u_R$ by a shock (contact discontinuity) propagating with speed $dx/dt = S_{M,R}$.

For the case in which $a(u_I)$ is a minimum, which is the case not considered in this paper, $S_{L,R} < a(u_L)$, $S_{L,R} < a(u_R)$, and the discontinuity is to the left, rather than to the right, of the expansion wave. The constructions above can complicate considerably for cases in which $f(u)$ has two or more inflections.

3.3. *Explicit Form of the Randomly Sampled Solution*

At time $t = \frac{1}{2}k$ we sample the Riemann solution $v(x, t)$ determined by the procedure of Section 3.2, at the spatial point $x = \frac{1}{2}\theta h$, where $\theta \in [-1, 1]$ is obtained by the random sampling procedure (iii) of [2] (see Section 4 below). The same value of θ is used for each spatial point of a given time step. We have

(a) If (Ia) occurs,

$$v(\tfrac{1}{2}\theta h, \tfrac{1}{2}k) = \begin{cases} u_L, & \text{if } \theta h/k \leqslant S_{L,R}, \\ u_R, & \text{if } \theta h/k > S_{L,R}. \end{cases} \tag{6a}$$

(b) If (Ib) occurs,

$$v(\tfrac{1}{2}\theta h, \tfrac{1}{2}k) = \begin{cases} u_L, & \text{if } \theta h/k \leqslant a(u_L), \\ u_R, & \text{if } \theta h/k > a(u_R), \\ u^* \text{ such that } a(u^*) = \theta h/k, & \text{if } a(u_L) < \theta h/k \leqslant a(u_R). \end{cases} \tag{6b}$$

(c) If (II) occurs,

$$v(\tfrac{1}{2}\theta h, \tfrac{1}{2}k) = \begin{cases} u_L, & \text{if } \theta h/k \leqslant a(u_L), \\ u_R, & \text{if } \theta h/k > S_{M,R} = a(u_M), \\ u^* \text{ such that } a(u^*) = \theta h/k, & \text{if } a(u_L) < \theta h/k \leqslant S_{M,R}. \end{cases} \tag{6c}$$

The value of u^* between u_L and u_R is the one to be taken in (6b), and the value between u_L and u_M is the one to be taken in (6c). Figures 3, 4, and 5 illustrate the different cases (6a), (6b), and (6c). Note, as depicted in the figures, that the disturbances from the discontinuities propagate a distance less than $\frac{1}{2}h$ during the time interval $\frac{1}{2}k$, in keeping with the Courant condition (4). The fan of characteristics corresponding to the family of solutions $u^*(\theta)$ of $a(u^*) = \theta h/k$ in (6b) and (6c), typical for an expansion wave, is illustrated in Figs. 4 and 5.

Note that it is straightforward with only a small amount of computational effort to determine whether case (Ia), (Ib), or (II) occurs and to calculate the corresponding solution of the Riemann problem from (6a), (6b), or (6c). In some cases it is not necessary to calculate both $f(u)$ and $a(u)$, and, in general, the most time-consuming calculations, those of solving $a(u_M) = S_{M,R}$ and $a(u^*) = \theta h/k$, will be required for only a fraction of the points at any time step. With an efficient root solver even these latter calculations can be accomplished with only a few function evaluations.

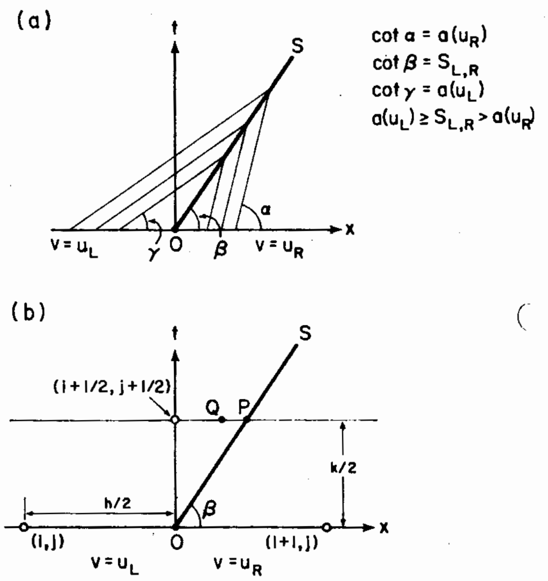

FIG. 3. Illustration of the Riemann problem solution (6a) for the case (Ia). (a) Characteristics from opposite sides of the discontinuity cross, developing a shock S. (b) In a local system of coordinates, O is the origin (0,0) and P has coordinates $(\frac{1}{2}S_{L,R}\,k, \frac{1}{2}k)$. The sampled point Q has coordinates $(\frac{1}{2}\theta h, \frac{1}{2}k)$, $-1 < \theta < 1$. If Q is to the left of P, then $v = u_L$, otherwise $v = u_R$.

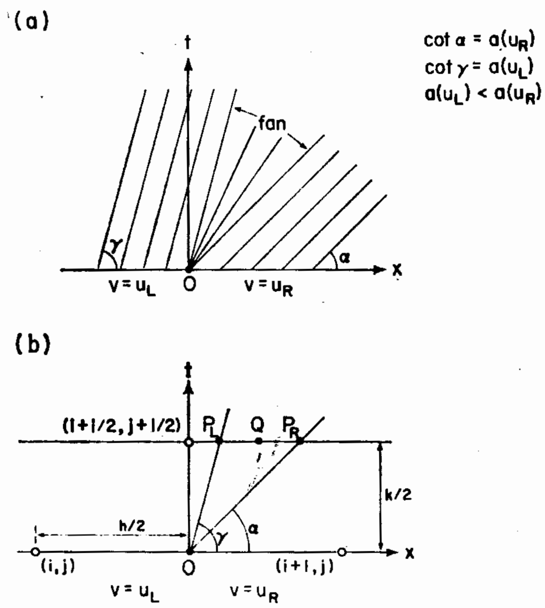

FIG. 4. Illustration of the Riemann problem solution (6b) for case (Ib). (a) Characteristics from opposite sides of the discontinuity diverge, giving an expansion wave, as illustrated by the fan of characteristics. (b) In a local system of coordinates, P_L is the point $(\frac{1}{2}a(u_L)k, \frac{1}{2}k)$ and P_R is the point $(\frac{1}{2}a(u_R)k, \frac{1}{2}k)$. The sampled point Q is $(\frac{1}{2}\theta h, \frac{1}{2}k)$. If Q is to the left of P_L, then $v = u_L$; if it is to the right of P_R, then $v = u_R$; otherwise the value of v is determined by solving the equation $a(v) = \theta h/k$.

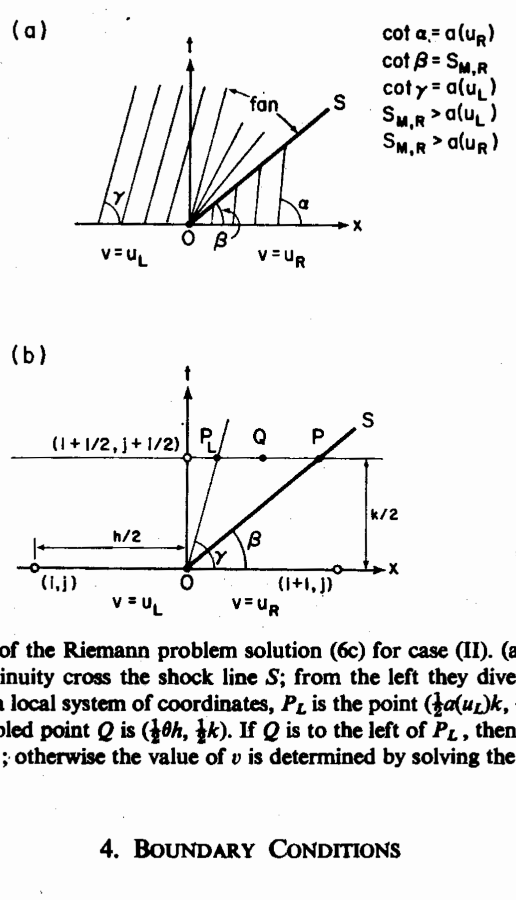

FIG. 5. Illustration of the Riemann problem solution (6c) for case (II). (a) Characteristics from the right of the discontinuity cross the shock line S; from the left they diverge from it, giving an expansion wave. (b) In a local system of coordinates, P_L is the point $(\frac{1}{2}a(u_L)k, \frac{1}{2}k)$, and P is the point $(\frac{1}{2}S_{M,R}\,k, \frac{1}{2}k)$. The sampled point Q is $(\frac{1}{2}\theta h, \frac{1}{2}k)$. If Q is to the left of P_L, then $v = u_L$; if it is to the right of P, then $v = u_R$; otherwise the value of v is determined by solving the equation $a(v) = \theta h/k$.

4. Boundary Conditions

In [2, 3] Chorin has shown that the accuracy and resolution of RCM are sensitive to the manner in which boundaries are treated. Correspondingly, he has developed the following sampling procedure.

Let $k_1 < k_2$ be mutually prime integers with k_2 odd, and let n_1 be an integer, $n_1 < k_2$. Construct the sequence of integers

$$n_{i+1} = (n_i + k_1) \qquad (\text{mod } k_2). \tag{7}$$

Then for the Riemann-problem solutions in the first half-step, use

$$\theta_{j+\frac{1}{2}} = (n_{2j+1} + \theta'_{j+\frac{1}{2}})/k_2 - 1 \tag{8a}$$

when sampling at time $t = (j + \frac{1}{2})k$, and in the second half-step use

$$\theta_{j+1} = (n_{2j+2} + \theta'_{j+1})/k_2 \tag{8b}$$

when sampling at time $t = (j + 1)k$, $j = 0, 1,\ldots$. The quantities $\theta'_{j+\frac{1}{2}}$ and θ'_{j+1} are selected at random from the uniform distribution on [0, 1]. With the above procedure, $\theta_{j+\frac{1}{2}}$ lies in a subinterval of $[-1, 0]$ and θ_{j+1} lies in a subinterval of [0, 1]. Chorin [3] has shown that this procedure prevents the loss of information at boundaries.

For the porous-flow problem, we wish to solve (1) on a finite interval $0 \leqslant x \leqslant (m + \frac{1}{2})h$. In the first half time step, from jk to $(j + \frac{1}{2})k$, the value of $u_{m+\frac{1}{2}}^{j+\frac{1}{2}}$ cannot be computed from values of u in the interval $0 \leqslant x \leqslant (m + \frac{1}{2})h$ at the previous time level, and similarly for u_0^{j+1} in the second half time step. According to the strategy in [2, 3] the values of u_{m+1}^j and $u_{-\frac{1}{2}}^{j+\frac{1}{2}}$ must first be obtained through the use of boundary conditions. For example, if the Dirichlet condition $u(0, t) = b_1$ is prescribed, then we set $u_{-\frac{1}{2}}^{j+\frac{1}{2}} = 2b_1 - u_{\frac{1}{2}}^{j+\frac{1}{2}}$, whereas if the Neumann condition $\partial u/\partial n\,|_{(0,t)} = b_2$ is prescribed, then we set $u_{-\frac{1}{2}}^{j+\frac{1}{2}} = u_{\frac{1}{2}}^{j+\frac{1}{2}} - b_2 h$, and similarly at a boundary on the right.

Note that for the porous-flow problem, since $a(u)$ is nonnegative, waves travel to the right, in general, as time increases, and it is appropriate to apply a boundary condition for (1) at the left end point, but not at the right. The sampling procedure (7) and (8) correctly ensures that for this case information travels across the boundary at $x = (m + \frac{1}{2})h$ only to the right, and the solution obtained by the algorithm is independent of values chosen for u_{m+1}^j. Note that if a Dirichlet condition (or a Neumann condition with zero data) is prescribed for this case at $x = 0$, then the end-point condition reduces simply to $u_0^j = u_0^0, j = 1, 2, \ldots$.

5. Multidimensional Problems

In [2] Chorin has indicated how to extend RCM to problems with more than one variable by means of a splitting technique. Fractional steps are taken by sweeping in each coordinate direction separately, in such a way that in the mean, the correct interaction of fractional waves is obtained. If the boundaries are parallel to the mesh, then generalization from a one-dimensional problem is straightforward. If some of the boundaries are oblique, then special procedures are required [2].

Consider the extension of RCM to the equation

$$\frac{\partial u}{\partial t} + \frac{\partial}{\partial x} f_1(u) + \frac{\partial}{\partial y} f_2(u) = 0$$

in two spatial variables on a domain with boundaries parallel to mesh lines. Each half-step in time is split into two consecutive sweeps: one in the x direction to solve $\partial u/\partial t + \partial f_1(u)/\partial x = 0$, followed by one in the y direction to solve $\partial u/\partial t + \partial f_2(u)/\partial y = 0$. Each sweep is carried out in the same manner as in the one-dimensional case. The boundary conditions are treated as described in Section 4 for each coordinate, with the other coordinate value fixed. If a value of $\frac{1}{2}$, instead of 1, is used on the right-hand side of (4), then the waves from the separate Riemann problems will not interact. One may choose a new value of θ for each sweep, as in [2], or, if symmetry considerations so require, keep θ fixed at a single value for both fractional sweeps of a given half-step in time.

6. Applications and Numerical Experiments

The simultaneous one-dimensional flow of two immiscible fluids through a porous medium in the absence of capillary pressure and gravitational forces can be described by the equation given by Buckley and Leverett in [1]. We consider the flow of oil and water through sand and denote by u the water saturation in the sand. Then the Buckley–Leverett equation is

$$\frac{\partial u}{\partial t} + \frac{Q}{\phi}\frac{\partial}{\partial x} f(u) = 0, \tag{9}$$

where $f(u) = [1 + \alpha k_0(u)/k_w(u)]^{-1}$ is the flux function of the flowing stream; $k_0(u)$ and $k_w(u)$ are the relative permabilities of sand to oil and to water, respectively; $\alpha = \mu_w/\mu_0$ is a constant, with μ_w and μ_0 the viscosities of water and oil, respectively; Q is the total flow; and ϕ is the porosity.

In two spatial dimensions the saturation equation is still a single nonlinear equation for the single unknown u, once the total velocity is determined [11]. Here we investigate the behavior of RCM for solving the saturation equation in one dimension, and in two dimensions for the case in which the total velocity is constant. In a subsequent study we intend to investigate the application of RCM to more complex multi-dimensional flows in a porous medium.

In (9), the flux function $f(u)$, which depends on the relative permeabilities $k_0(u)$ and $k_w(u)$, is such that the assumptions of Section 3.2 are satisfied. That is, $df(u)/du$ is nonnegative and has exactly one interior maximum [10]. It is known from physical observation that sharp fronts occur in the spatial distribution of u [1].

Several numerical methods have been used previously to solve (9), but none have proved to be completely satisfactory. Finite-difference methods employ exceedingly small time steps, resulting in excessive computational requirements [10, 11]. Recently, a variational method has been developed, which has the ability of tracking sharp fronts [12]; however, it requires the presence of a capillary-pressure term.

We report here on the results of our numerical experiments with the model flux function $f(u)$ (see [12])

$$\begin{aligned} f(u) &= \frac{u^2}{u^2 + \alpha(1-u)^2}, \\ \frac{df}{du} &= a(u) = \frac{2\alpha u(1-u)}{[u^2 + \alpha(1-u)^2]^2}. \end{aligned} \tag{10}$$

The domain of interest is $0 \leqslant u \leqslant 1$, and we take $\alpha = \frac{1}{2}$ and $Q/\phi = 1$. The values chosen in (8) are $k_1 = 3$ and $k_2 = 7$.

For the solutions of the one-dimensional problems depicted in Figs. 6 and 7, u is plotted at every $k_2 = 7$ time steps. The space and time increments are $h = 0.02$ and $k = 0.009$, for which (4) is satisfied. For the first example, depicted in Fig. 6, the initial distribution is $u(x, 0) = 0.05$ for $x > 0$, and $u(0, t) = 0.55$ for $t \geqslant 0$. For this choice $a(u_L) > S_{L,R} > a(u_R)$ holds at the discontinuity for all $t \geqslant 0$, and the

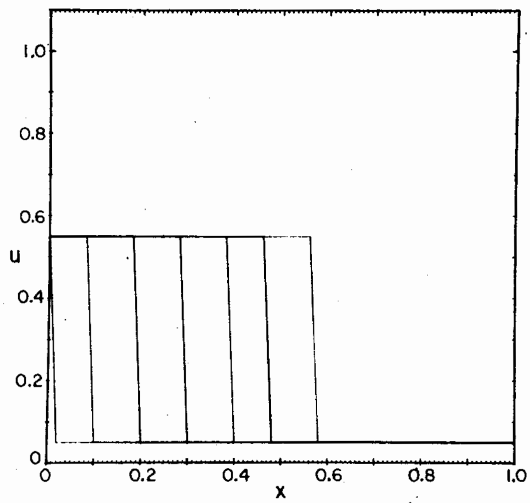

FIG. 6. A one-dimensional problem. The initial distribution is $u(x, 0) = 0.05$ for $x > 0$, and $u(0, t) = 0.55$. The solution $u(x, t)$ at every $k_1 = 7$ time steps is plotted. The wave is a pure shock for all $t > 0$.

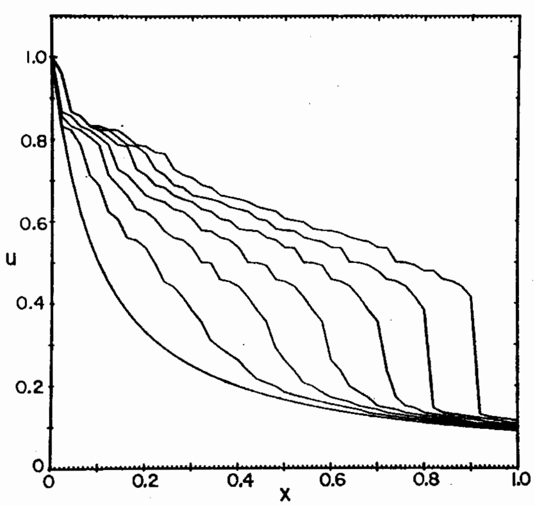

FIG. 7. A one-dimensional problem. The initial distribution is $u(x, 0) = 0.1/(x + 0.1)$, and $u(0, t) = 1.0$. The solution $u(x, t)$ at every $k_1 = 7$ time steps is plotted.

exact solution of (1) is a shock traveling to the right with speed $S_{L,R}$. As shown in Fig. 6, the initial discontinuity is propagated by the RCM method sharply, without changes. (The nonvertical shock fronts result from the linear interpolation between mesh values in the plotting routine.) The average value 1.48 of the shock speed obtained from this numerical experiment is in good agreement with the exact value $S_{L,R} \cong 1.49$.

For the second example, depicted in Fig. 7, the initial distribution is $u(x, 0) =$

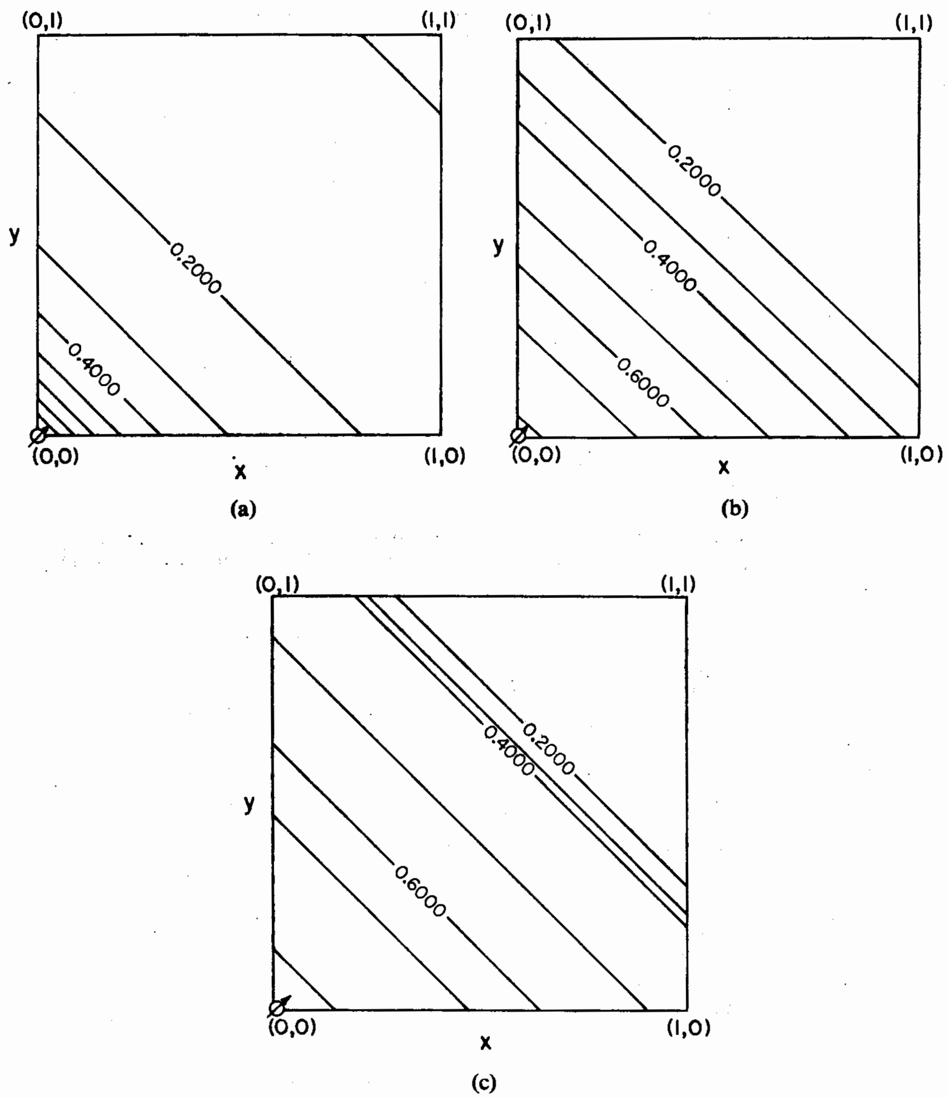

FIG. 8. A two-dimensional problem. (a) Contours of $u(x, y; t)$ for $t = 0$ (initial distribution). (b) Contours of $u(x, y; t)$ after $k_2 = 7$ time steps. (c) Contours of $u(x, y; t)$ after $2k_2 = 14$ time steps.

$0.1/(x + 0.1)$, with $u(0, t) = 1.0$ for $t \geqslant 0$. Here the situations shown in Figs. 3–5 all occur. Even for this case, a sharp front develops and is tracked by the algorithm without difficulty. Carrying out a typical time step (two half-steps) on the CDC-7600 computer required approximately $1\frac{1}{2}$ msec for our FORTRAN program using an FTN4 (OPT = 2) compiler.

For a two-dimensional example we solve

$$\frac{\partial u}{\partial t} + \frac{\partial}{\partial x} f(u) + \frac{\partial}{\partial y} f(u) = 0$$

on a square, with $f(u)$ given by Eq. (10). The initial distribution is taken to be $u(x, y; 0) = 0.2/(x + y + 0.2)$, for which the contours of u, $u(x, y; 0) = \text{const}$, run diagonally across the square. The boundary condition is that the directional derivative $\partial u/\partial s$ is equal to zero, where s is arc length along a contour of u. At $(0, 0)u$ is kept fixed at the value 1. For a uniform spacing h in x and y, the boundary conditions are discretized naturally as $u(-\frac{1}{2}h, y; [j + \frac{1}{2}]k) = u(\frac{1}{2}, y - h; [j + \frac{1}{2}]k)$, and similarly at the other boundary points. The same value of θ is used for both the x and y sweeps at each time step, so that the property that u depends only on $x + y$ is preserved. The solution is thus one dimensional in nature, but at an angle of $\frac{1}{4}\pi$ with the coordinate axes. The values of h and k are chosen to satisfy (4) with $\frac{1}{2}$ on the right-hand side.

In Figs. 8a–c, the solutions after 0, 7, and 14 time steps are plotted. The region in which the contours are closely drawn represents a sharp front. The smoothness with which this front advances demonstrates the ability of the method to track it, similar to the case in Fig. 7. The number of mesh points in the x-y plane is 21×21. On the average our program required approximately 20 msec to carry out a typical time step (two half-steps) for this problem.

The function $a(u)$ in Eq. (10) is depicted in Fig. 9. Subroutines LINESG and CONREC from the NCAR graphics package were used for plotting Figs. 6–9.

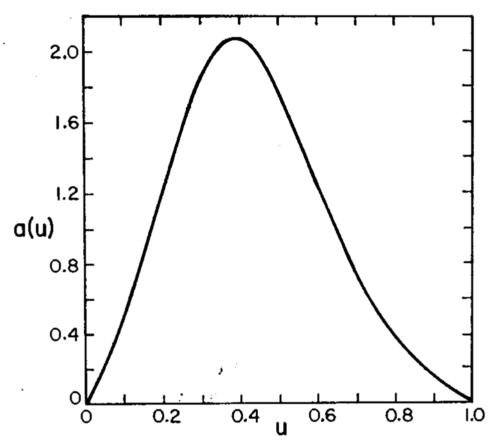

FIG. 9. The function $a(u)$ in (10).

ACKNOWLEDGMENTS

We wish to thank Alexandre Chorin for his invaluable and illuminating advice on the random choice method. We wish also to thank the referees for their constructive comments; those of Gerald

Hedstrom were particularly helpful for improving the presentation in Section 3. Discussions with Philip Colella and Charles Fenimore are also acknowledged. We first learned of the porous-flow problem during the Gordon Research Conference on Fluids in Permeable Media, in August 1976, and are indebted to Paul Saylor and Donald Peaceman for providing us further references and for their encouragement. This work was carried out under the auspices of the U.S. Department of Energy.

REFERENCES

1. S. E. BUCKLEY AND M. C. LEVERETT, *Trans. AIME* **146** (1942), 107–116.
2. A. J. CHORIN, *J. Comput. Phys.* **22** (1976), 517–533.
3. A. J. CHORIN, *J. Comput. Phys.* **25** (1977), 253–272.
4. C. M. DAFERMOS, *J. Math. Anal. Appl.* **38** (1972), 33–41.
5. J. GLIMM, *Comm. Pure Appl. Math.* **18** (1965), 697–715.
6. N. N. KUZNECOV AND V. A. TUPČIEV, *Soviet Math. Dokl.* **16** (1975), 340–343.
7. P. D. LAX, *Comm. Pure Appl. Math.* **10** (1957), 537–566.
8. P. D. LAX, Hyperbolic systems of conservation laws and the mathematical theory of shock waves, SIAM Regional Conference Series in Applied Mathematics, 1973.
9. O. A. OLEĬNIK, *Amer. Math. Soc. Transl. Sec. 2* **33** (1963), 285–290.
10. D. W. PEACEMAN, Numerical solution of the nonlinear equations for two-phase flow through porous media, *in* "Nonlinear Partial Differential Equations" (W. F. Ames, Ed.), Academic Press, New York, 1967.
11. D. W. PEACEMAN, "Fundamentals of Numerical Reservoir Simulation," Elsevier, Amsterdam, 1977.
12. A. SPIVAK, H. S. PRICE, AND A. SETTARI, *Soc. Pet. Eng. J.* **17** (1977), 27–41.

Printed by the St Catherine Press Ltd., Tempelhof 37, Bruges, Belgium.